A Telepresence Mobile Robot Controlled With a Noninvasive Brain–Computer Interface

Carlos Escolano, Javier Mauricio Antelis, and Javier Minguez

Abstract—This paper reports an electroencephalogram-based brain-actuated telepresence system to provide a user with presence in remote environments through a mobile robot, with access to the Internet. This system relies on a P300-based brain–computer interface (BCI) and a mobile robot with autonomous navigation and camera orientation capabilities. The shared-control strategy is built by the BCI decoding of task-related orders (selection of visible target destinations or exploration areas), which can be autonomously executed by the robot. The system was evaluated using five healthy participants in two consecutive steps: 1) screening and training of participants and 2) preestablished navigation and visual exploration telepresence tasks. On the basis of the results, the following evaluation studies are reported: 1) technical evaluation of the device and its main functionalities and 2) the users' behavior study. The overall result was that all participants were able to complete the designed tasks, reporting no failures, which shows the robustness of the system and its feasibility to solve tasks in real settings where joint navigation and visual exploration were needed. Furthermore, the participants showed great adaptation to the telepresence system.

Index Terms—Brain computer interfaces, rehabilitation robotics, telerobotics.

I. INTRODUCTION

BRAIN–COMPUTER interfaces (BCIs) provide users with communication and control using only their brain activity. BCIs do not rely on the brain's normal output channels of peripheral nerves and muscles, opening a new valuable communication channel for people with severe neurological or muscular diseases, such as amyotrophic lateral sclerosis (ALS), brain-stem stroke, cerebral palsy, and spinal cord injury. The ability to work with noninvasive recording methods (the electroencephalogram or EEG is the most popular method) is one of the major goals for the development of brain-actuated systems for humans. Some examples of EEG-based applications include the control of a mouse on a computer screen [1], communication such as spellers [2], Internet browsers [3], etc. The first noninvasive brain-actuated control of a physical device

The authors are with the Instituto de Investigación en Ingeniería de Aragón and the Departamento de Informática e Ingeniería de Sistemas, Universidad de Zaragoza, 50014 Zaragoza, Spain (e-mail: cescolan@unizar.es; antelis@unizar.es; jminguez@unizar.es).

was demonstrated in 2004 [4], and since then, research has been mainly focused on wheelchairs [5]–[8], manipulators [9], [10], small-size humanoids [11], and orthosis operated with functional electrical stimulation [12], [13], to name a few. All these developments have a property in common: user and robot are placed in the same environment.

Very recent research has focused on BCI applications where the human and the robot are not colocated, such as in robot teleoperation. Some examples include a museum guide robot [14], the teleoperation of a manipulator robot [9], an aircraft [15], or mobile robots [16], [17]. The ability to brain-teleoperate robots in a remote scenario could provide severely disabled patients with telepresence. Telepresence could be seen as an extension of the sensorial functions of daily life by means of a physical device, embodied in the real environment and placed anywhere in the world, which could perceive, explore, manipulate, and interact with the remote scenario, and controlled only by brain activity. Furthermore, it has been suggested that the use of these BCIs could have a neurorehabilitation effect and/or a maintenance of neural activity, avoiding or delaying the extinction of thought, hypothesized to occur in patients like ALS [18].

There are three major engineering problems in the design of this type of systems: 1) Current noninvasive BCIs are slow and uncertain; 2) BCIs when used as input interfaces are highly cognitive demanding; and 3) the variable and uncertain communication time delays in any development involving robot teleoperation via the Internet. For these reasons, research works have started to look at these systems from a shared-control point of view, where the robot is equipped with a degree of intelligence and autonomy that totally or partially manages the task (alleviating the previous problems). This principle was initially explored in the context of BCI control of wheelchairs [5], [6], [19] and very recently applied to BCI telepresence [17]. This paper is in line with these works.

The present BCI telepresence system relies on a synchronous P300-based BCI and a mobile robot with autonomous navigation and camera orientation capabilities (see [20] for reviews on BCIs and [21] on navigation systems). During operation, the user concentrates on the desired option on a computer screen, which displays live video sent by the robot along with relevant information related to robot motion or camera orientation tasks. Following the typical P300 visual stimulation processes, the BCI collects the EEG brain activity and decodes the user's intentions, which are transferred to the robot via the Internet. The robot autonomously executes the orders using the navigation system (implemented with a combination of dynamic online grid mapping with scan matching, dynamic path planning, and obstacle avoidance) or the camera orientation system. Thus, the

shared-control strategy is built by means of the mental selection of robot navigation or active visual exploration task-related orders, which can be autonomously executed by the robot. In principle, this shared-control design shapes the low information transfer rates (ITRs) of existing BCIs, avoids the exhausting mental effort of BCIs that require continuous control, and overcomes the Internet delay problems in the control loop. In relation to the shared-control approach used in [17] to teleoperate a mobile robot, which relies on a motor imagery BCI and low-level robot motion primitives, the contribution of the present engineering system is a shared-control design that incorporates a much higher degree of autonomy in the robotic layer.

An added value of this research is the experimental methodology and validation protocol, which could guide future developments. The telepresence system was evaluated using five healthy participants in two consecutive steps: 1) screening and training of participants and 2) preestablished navigation and visual exploration tasks performed during one week between two laboratories located 260 km apart. On the basis of the results, the following analyses are reported: 1) technical evaluation of the device and its main functionalities and 2) the users' behavior study. The overall result was that all participants were able to complete the designed tasks, reporting no failures, which shows the robustness of the system and its feasibility to solve tasks in real settings where joint navigation and visual exploration are needed. Furthermore, the participants showed great adaptation to the system.

In relation to our previous work, partial results were outlined in [22]. This paper reports the complete results of the investigation and is organized as follows: Section II describes the brain-actuated telepresence technology, Section III describes the experimental methodology, Section IV reports the results and evaluations, and conclusions are drawn in Section V.

II. TELEPRESENCE TECHNOLOGY

The telepresence system consisted of a user station and a robot station, both remotely located and connected via the Internet (Fig. 1). At the user station, the BCI decodes the user's intentions, which are transferred to the robotic system via the Internet. At the robot station, the user's decisions are autonomously executed using autonomous navigation and active visual exploration capabilities. Furthermore, the robot station provides live video (captured by the robot camera), which is used by the user as visual feedback for decision making and process control. From an interactional point of view, the user can switch between two operation modes: 1) robot navigation mode and 2) camera exploration mode. According to the operation mode, the graphical interface displays a set of augmented reality locations to navigate to or visually explore. The user then concentrates on the desired location, and a visual stimulation process elicits the P300 visual-evoked potential enabling the pattern-recognition strategy to decode the desired location. Finally, the target location is transferred to the robotic system via the Internet, which autonomously executes the relevant orders: 1) In the robot navigation mode, the autonomous navigation system drives the robot to the target location while avoiding collisions with obstacles detected by its laser sensor, and 2) in the
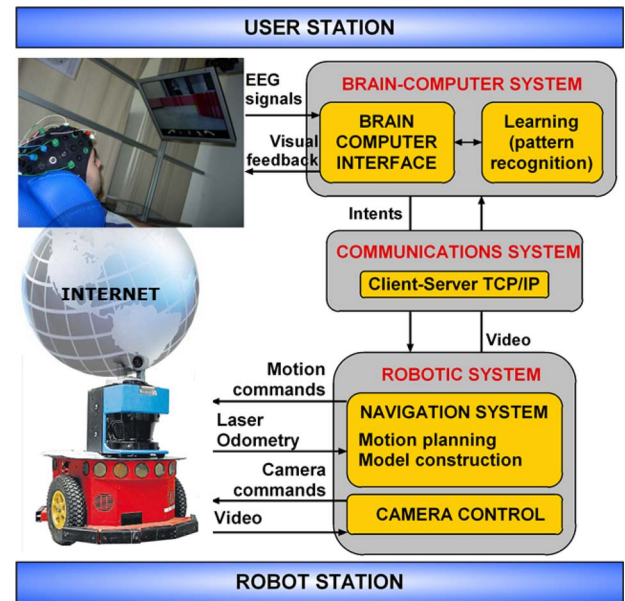

Fig. 1. Design of the robotic telepresence system actuated by a noninvasive BCI with main modules and information flow.

camera exploration mode, the camera is oriented to the target location, performing a visual exploration of the environment.

The next sections outline the three main modules that compose the global system: brain–computer system (protocol and EEG acquisition, graphical interface, and pattern-recognition strategy), robotic system, and integration between the systems.

A. BCI: Protocol and EEG Acquisition

The BCI was based on the P300 visual-evoked potential [23]. In this protocol, the user attends to one of the possible visual stimuli, and then, the brain–computer system detects the elicited potential in the EEG. The P300 potential is characterized by a positive deflection in the EEG amplitude at a latency of approximately 300 ms after the target stimulus is presented within a random sequence of nontarget stimuli [Fig. 2(a) and (b)]. Elicitation time and amplitude are correlated to fatigue of the user and to saliency of stimulus (color, contrast, brightness, etc.) [24]. This potential is always present as long as the user is attending to the process, and its variability among users is relatively low. BCIs based on this potential have been successfully used in patients for long periods of time in different assistive applications (see review in [25]).

EEG was acquired using a commercial gTec EEG system (EEG cap, 16 electrodes, and a gUSBamp amplifier). The electrodes were located at Fp1, Fp2, F3, F4, C3, C4, P3, P4, T7, T8, CP3, CP4, Fz, Pz, Cz, and Oz, according to the international 10/20 system, as suggested in previous studies [26]. The ground electrode was positioned on the forehead (position Fpz), and the reference electrode was placed on the left earlobe. The EEG was amplified, digitalized with a sampling frequency of 256 Hz, power-line notch filtered, and bandpass filtered between 0.5 and 30 Hz. Graphical interface and signal recording and processing were developed through the BCI2000 platform [27], placed on an Intel Core2 Duo processor at 2.10 GHz with Windows XP operating system (OS).
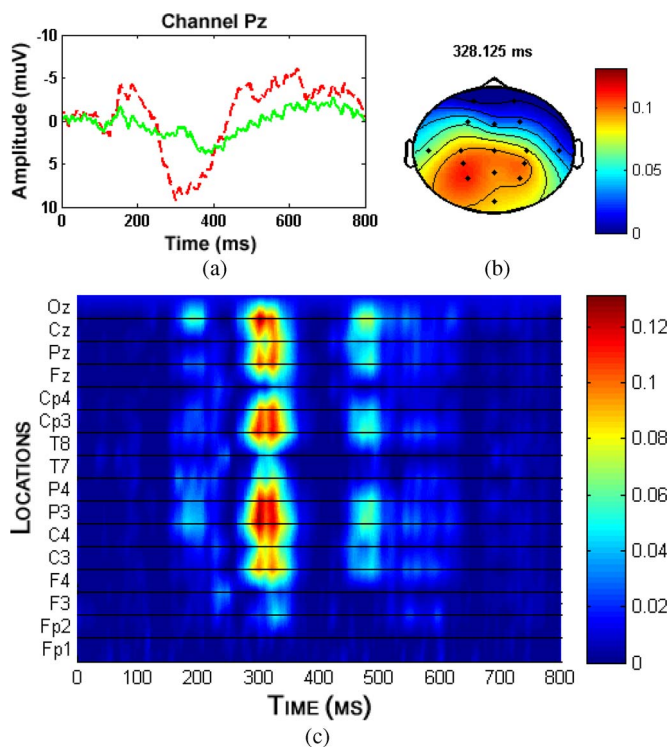
Fig. 2. (a) Grand average of the P300 response. The dashed line is the averaged EEG activity on Pz elicited by the target stimulus, and the solid line is the averaged EEG for the nontarget stimuli. (b) Topographical plot of the distribution of r^2 values on the scalp at 300 ms. r^2 indicates the proportion of single-trial signal variance due to the desired target [27]. (c) r^2 values for each location in an interval of 0–800 ms after the onset of stimulus target. Values are displayed in a color scale (higher values are found at a latency of approximately 300 ms).
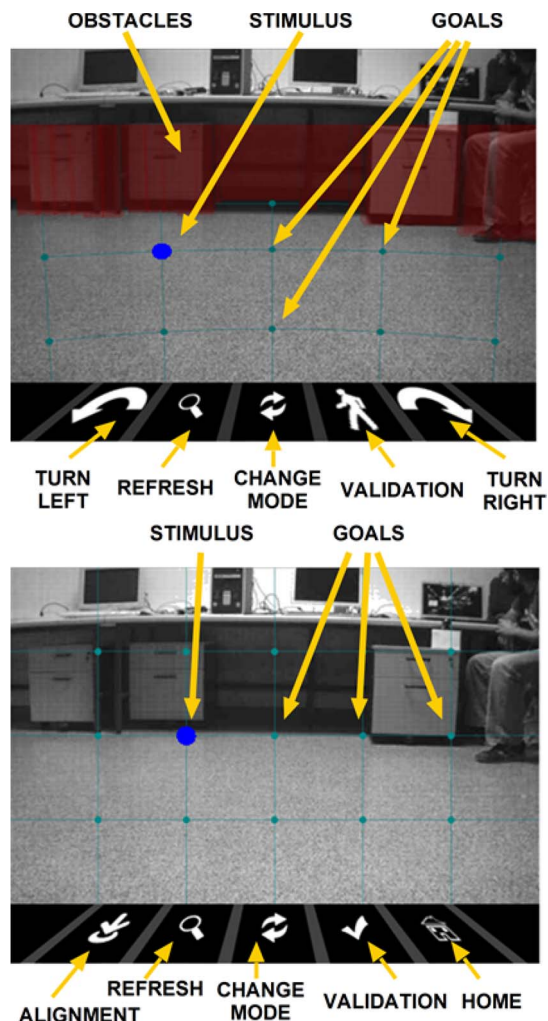

Fig. 3. Visual display (upper section of the figure) in robot navigation mode and (lower section of the figure) in camera exploration mode. An individual visual stimulus represented by a blue circle is shown in both figures; however, the real stimulation process was accomplished by means of rows and columns.

B. BCI: Graphical Interface

The brain–computer system incorporated a graphical interface with two functionalities: 1) to provide the user with the functionalities to control the robot and visual feedback of the robot environment and 2) to develop the visual stimulation process to trigger the P300 potentials.

a) Visual Display: In both operation modes (robot navigation and camera exploration), the visual display showed an augmented reality reconstruction of the robot environment overlapped with live video background (Fig. 3). The reconstruction displayed a predefined set of options, arranged in a 4×5 matrix to favor the next pattern-recognition strategy. In the robot navigation mode, a set of possible destinations was represented by a $(1.5\text{ m}, 2.5\text{ m}, 4\text{ m}) \times (-20°, -10°, 0°, 10°, 20°)$ polar grid referenced on the robot. Destinations were selected as a compromise between utility and good visualization and represented real locations in the environment that the user could select. Obstacles were depicted as semitransparent walls built from a 2-D map constructed in real time by the autonomous navigation technology, hiding unreachable destinations. The row of icons in the lower part of the display represented the following options, from left to right: 1) turn the robot 45° to the left; 2) refresh option; 3) change to camera exploration mode; 4) validate the previous selection; and 5) turn the robot 45° to the right. In the camera exploration mode, destinations were uniformly placed on a 2-D grid, which mapped a set of locations that the

user could select to orientate the camera in that direction. The row of icons in the lower part of the display represented the following options, from left to right: 1) align the robot with horizontal camera orientation and change to robot navigation mode; 2) refresh option; 3) change to robot navigation mode; 4) validate the previous selection; and 5) set the camera to its initial orientation. The refresh option allowed the user to receive live video for 20 s, freezing the stimulation process in that interval. Further information on an improved version of the present visual display, which incorporates bidirectional communication along the lines of a video conference, can be found in [28].

b) Stimulation Process: A visual stimulation process was designed to elicit the P300 visual-evoked potential. The options of the visual display were "stimulated" by flashing a circle on them. The Farwell and Donchin paradigm [29] was followed to reduce the magnitude of the posterior classification problem and sequence duration (a sequence is a stimulation of all options in a random order as required by the P300 oddball paradigm). Flashing of stimulus was accomplished by means of rows and columns instead of flashing each option individually, obtaining 9 stimulations per sequence (4 rows plus 5 columns) instead of 20.

All visual aspects of the elements shown on the visual display (color, texture, shape, size, and location) as well as all scheduling of the stimulation process (mainly stimulus duration, interstimulus interval, and number of sequences) could be customized to equilibrate the user's capabilities and preferences with the performance of the system. Note that the P300 potential is correlated to these aspects.

C. BCI: Pattern-Recognition Strategy

A supervised pattern-recognition technique was used to recognize the P300 visual-evoked potential. This technique was applied offline to previously recorded EEG, where the user attends to a predefined sequence of targets. The technique consisted of two steps: 1) feature extraction and 2) classification algorithm.

a) Feature Extraction: In order to extract features, EEG data were first preprocessed following the technique described by Krusienski *et al.* [26]: 1-s vectors of data were extracted after each stimulus onset for each EEG channel, and these segments of data were then filtered using the moving average technique and downsampled by a factor of 16. Selection of input channels for the classifier was based on the r^2 metric [27]. For each channel, this metric computes the variance between target and nontarget feature vectors (note that each feature vector could be labeled as target or nontarget according to whether the stimulus was attended to or not by the user). Thus, r^2 values for each channel were plotted [Fig. 2(c)], and the channels with higher r^2 were selected through visual inspection (*a priori*, those channels will be the best to discriminate through a linear classifier). Finally, following the study of Krusienski *et al.* [26] again, the feature vectors of selected channels were normalized and concatenated, creating a single-feature vector for the classification algorithm.

b) Classification Algorithm: Two classification subproblems were obtained following the adoption of the Farwell and Donchin paradigm in the stimulation process. The StepWise Linear Discriminant Analysis (SWLDA) was used for each subproblem. SWLDA is an extension of the Fisher linear discriminant analysis (FLDA), which performs a reduction in the feature space by selecting the most suitable features to be included in a discriminant function. This classification algorithm has been extensively studied for P300 classification problems, obtaining very good results in online communication using visual stimulation [30].

The P300 signal-to-noise ratio is low, but it can be improved by averaging the responses through repetitions of the stimulation process (number of sequences). This leads to higher classification accuracy at the cost of longer stimulation time (time of a sequence in the stimulation process is approximately 2 s). The number of sequences is usually customized per user (Fig. 4).

D. Autonomous Robotic System

The robot was a commercial *Pioneer P3-DX*, equipped with a laser sensor, a camera, back wheels (working in a differential-drive mode), wheel encoders (odometry), and a network interface card. The main sensor was a *SICK* planar laser placed on
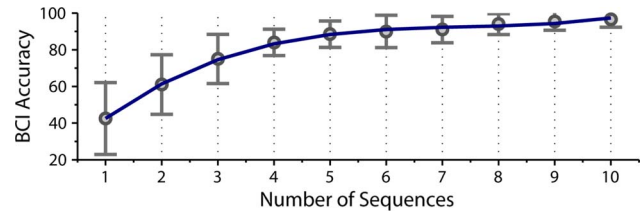

Fig. 4. BCI classification accuracy versus the number of sequences of the stimulation process. Mean and standard deviation values are shown for all the participants in the calibration trials of the *evaluation of brain-actuated telepresence* (see methodology). Tenfold cross-validation was applied.
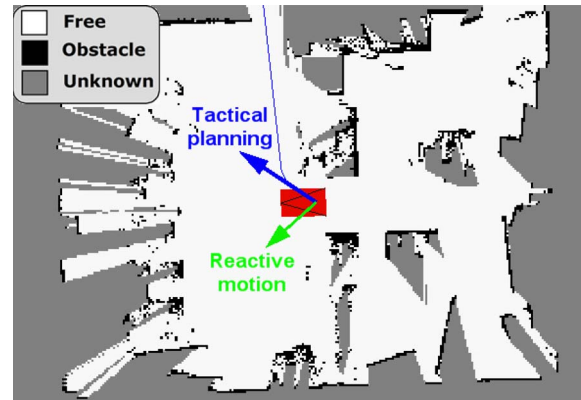

Fig. 5. Execution trace of the navigation system: Static model (free, obstacle, and unknown space), tactical planning direction (obtained from the dynamic-path-planning strategy), and direction solution of the obstacle avoidance.

the frontal part of the robot; the laser operated at a frequency of 5 Hz with a $180°$ field of view and a $0.5°$ resolution (361 points). The camera, placed on the laser, was a pan/tilt *Canon VC-C4* camera with a $\pm100°$ pan field of view and a $90°/-30°$ tilt field of view. The robot was equipped with a computer with an Intel processor at 700 MHz with Linux OS (Debian distribution). The computer managed all computational tasks, provided access to the hardware elements through the *player* robot device interface [31], and integrated the autonomous navigation system. In the experiments, the maximum translational and rotational velocities were set to 0.3 m/s and 0.7 rad/s, respectively. The objective of the autonomous navigation system was to drive the vehicle to a given destination, set by the BCI, while avoiding obstacles detected by the laser sensor. The general assumption is that the environment is unknown and dynamic (it can vary with time), which imposes a difficulty since precomputed maps and trajectories cannot be used. To deal with this problem, the navigation system implemented online modeling and dynamic planning capabilities [32], integrated into two modules: the model builder and the local planner (Fig. 5).

a) Model Builder: The model builder integrates sensor measurements to construct a local model of the environment (static and dynamic parts) and to track the vehicle's location. Free space and static obstacles are modeled by a ternary occupancy map. Dynamic objects are tracked using a set of extended Kalman filters. In order to accurately build both models, a technique is used to correct the robot's position, update the map, and detect and track the moving objects around the robot [32]. The static map travels centered on the robot. This map has a limited but sufficient size to present the required information to

the user (as described in the graphical interface section) and to compute the path so as to reach the selected target destination.

b) Local Planner: The local planner computes the local motion based on the hybrid combination of tactical planning and reactive collision avoidance [33], [34]. An efficient dynamic navigation function (D*Lite planner [35]) is used to compute the tactical information (i.e., main direction of motion) required to avoid cyclic motions and trap situations. This function is well suited for unknown and dynamic scenarios because it works based on the changes in the model computed by the model builder. The final motion of the vehicle is computed using the Nearness Diagra technique [36], which uses a case-based strategy, based on situations and actions to simplify the collision avoidance problem. This technique has the distinct advantage that it is able to deal with complex navigational tasks such as maneuvering in the environment within constrained spaces (e.g., passage through a narrow doorway). In order to facilitate comfortable and safe operation during navigation, shape, kinematics, and dynamic constraints of the vehicle are incorporated [37].

E. Integration Platform and Execution Protocol

The communication system performed the integration between the brain–computer system and the robotic system. The software architecture was based on the Transmission Control Protocol/IP and the client/server paradigm. It consisted of two clients (one for the brain–computer system and one for the robotic system) plus a link server that concentrated information flow and conferred scalability to the system. This design allows for teleoperation of the robot in any remote environment via an Internet connection. The BCI client was integrated within the BCI2000 platform [27], cyclically executed every 30 ms, and communicated with the link server through an Internet connection. The robot client encapsulated the navigation system, synchronized the orders to the camera and to the navigation system, and communicated with the link server through a peer-to-peer (*ad hoc*) wireless connection. This client also communicated with the robot hardware controllers using the *player* robot device interface [31]. Regarding the hardware components, the BCI client operated in a computer executing all the BCI software. The link server operated in a dedicated computer, with an Intel Core2 Duo processor at 2.10 GHz with Linux OS (Ubuntu distribution), equipped with an Ethernet and wireless network card. The robot client operated in the computer embedded in the robot. The autonomous navigation system was a time-critical task, which was integrated in the robot computer within a thread-based system with time-outs to preserve the computation cycle (200 ms).

A typical execution of a navigation order is described next. The BCI infers the user desired goal location (8 B of information), which is transferred via the Internet from the BCI client to the link server. The link server transfers the goal location to the robot client via the *ad hoc* wireless connection. The robot client makes the location available to the navigation system. Within a synchronous periodical task of 200 ms, the navigation system reads the location of the robot from the motor control system and the laser sensor, requests the robot

odometry, executes the mapping and planning module, and sends the computed translational and rotational velocities to the robot controllers. While the robot is navigating, the robot client iteratively requests images from the camera, which are transferred to the BCI. Finally, when the robot reaches the final location, the navigation system triggers a flag to stop the image transfer process and sends three variables to the BCI to display the reconstruction of the environment: the map model (400 B), the model location (12 B), and the robot location within the map (12 B). The upper boundary of the information transfer was set by the video transfer rate. The images captured by the camera were compressed to the *jpeg* standard format, obtaining an image size of approximately 30 kB. In the experimental sessions, ten images per second were transferred, resulting in a transfer rate of approximately 300 kB/s, which is adequate for the typical bandwidth order of Internet networks.

a) Execution Protocol: The way that the users interact with the system is modeled by a finite-state machine with three states: *Selection*, *Validation*, and *Execution*. Initially, the state is *Selection*, and the BCI develops the stimulation process while the robotic system is in an idle state. Then, the BCI selects an option, and the state changes to *Validation*. In this state, a new stimulation process is developed, and the BCI selects a new option. Only when the selected option is validation that the previous selection is transferred to the robotic system, and the state changes to *Execution*. In this state, the robotic system executes the order (this will be referred as a mission). While the robot is executing the mission, the BCI is in an idle state (no stimulation process is developed), and the live video captured by the robot camera is sent to the graphical interface. Once the robot accomplishes the mission, the state turns to *Selection*, video transfer stops (no interference stimuli, which could decrease BCI accuracy), and the BCI stimulation process starts again. Note that the validation option reduces the probability of sending incorrect orders to the robotic system, as BCI is always an uncertain channel.

III. EXPERIMENTAL METHODOLOGY

An experimental methodology was defined to carry out a technical evaluation of the system and to assess the degree of user adaptability. The experimental sessions were performed by healthy users in real settings. The recruitment of the participants and the experimental protocol are discussed next.

A. Participants

Inclusion and exclusion criteria were defined in order to obtain conclusions over a homogeneous population. The inclusion criteria are as follows: 1) users within the age group of 20–25 years of age; 2) gender (either all women or all men); 3) laterality (either all left-handed or all right-handed); and 4) students of the Universidad de Zaragoza. The exclusion criteria are as follows: 1) users with history of neurological or psychiatric disorders; 2) users under any psychiatric medication; and 3) users with episodes of epilepsy and dyslexia or experiencing hallucination. Five healthy 22-year-old male right-handed students of the Universidad de Zaragoza were
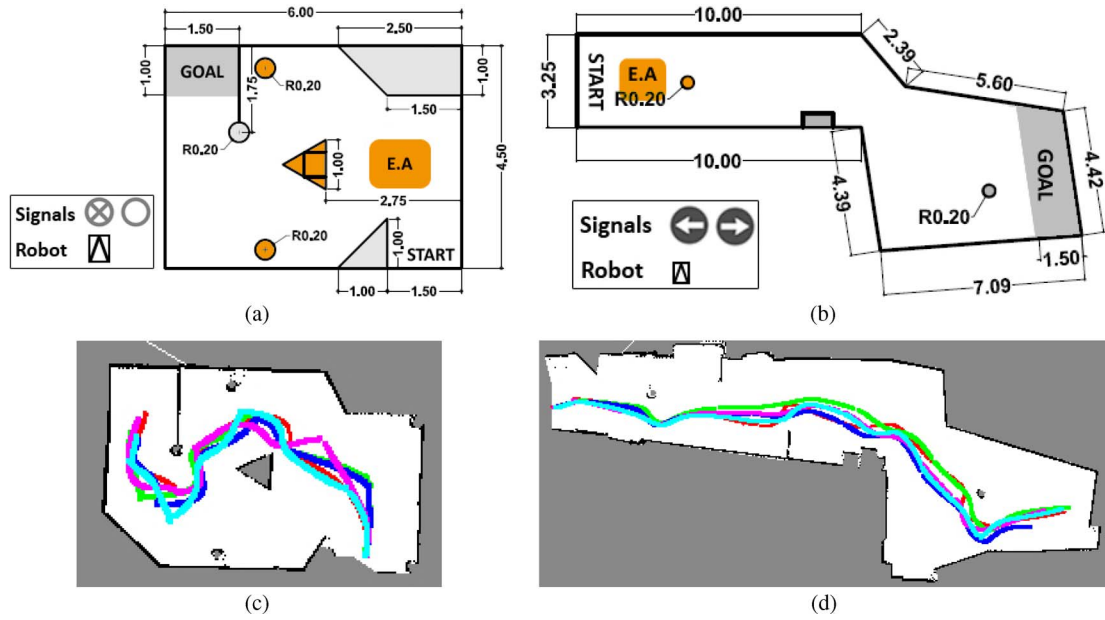
Fig. 6.   (a) Objective of Task 1 was to drive the robot from the *start* location to the *goal* area. In the exploration area (E.A. in the figure), the participant had to search for two signals located on the yellow cylinders 2.5 m above the floor. If both signals were equal, the participant had to avoid the yellow triangle by turning to the right, and if the signals were different, the participant had to turn to the left. (b) Objective of Task 2 was to drive the robot from the *start* location to the *goal* area. In the exploration area, the participant had to search for one signal located in the yellow cylinder 2.5 m above the floor. The participant then had to continue navigating to the right or left of the two cylinders, as specified by the signal. All measurements are in meters, and the robot is to scale. (c and d) Maps generated by the autonomous navigation system (black zones indicate obstacles, white zones indicate known areas, and gray zones indicate unknown areas). The trajectories of the robot for one trial per participant are shown. (a) Task 1. (b) Task 2. (c) Task 1 trajectories. (d) Task 2 trajectories.

recruited. They had neither utilized the telepresence system nor participated in BCI experiments before. The study was approved by the Universidad de Zaragoza's Institutional Review Board. All participants signed informed consents after being informed about the entire protocol.

B. Experiment Design and Procedures

The study was divided into two phases: 1) screening and training phase and 2) a brain-actuated telepresence phase. Both phases were carried out in the BCI Laboratory of the Universidad de Zaragoza on different days.

1) Evaluation of Screening and Training: This phase consisted of two tasks: 1) screening task to study the P300 response and validate the graphical interface design and 2) training task to calibrate the system and measure the BCI accuracy. Initially, the visual aspects of the graphical interface were selected adapting the results of a parallel study [5]. Images were captured in black and white to preserve high saliency of stimuli; the initial camera orientation was $0°$ pan and $-11.5°$ tilt to provide a centered perspective of the environment starting approximately 1 m in front of the robot. The final aesthetic factors of the visual display are shown in Fig. 3. Stimulation process schedules were also set for both tasks according to Iturrate *et al.* [5]. The interstimulus duration was set to 75 ms, and the stimulus duration was set to 125 ms.

The screening task consisted of eight offline trials to study the P300 response in the EEG. In each trial, the participants had to attend to a predefined sequence of ten targets. After execution, participants were asked to fill out neuropsychological and cognitive assessment forms. The training task consisted of

a battery of online tests (facing the graphical interface without teleoperating the robot) to check whether the accuracy of the system was greater than a threshold value of 90%, qualifying the participant for the next phase. The duration of this phase was 3 h per participant.

2) Evaluation of Brain-Actuated Telepresence: This phase consisted of a battery of online experiments with the telepresence system in order to carry out a technical evaluation of the system and to assess the degree of user adaptability. The experiments were carried out between the BCI Laboratory at the Universidad de Zaragoza (Spain) and the University of Vilanova i la Geltrú (Spain), separated by 260 km. Two tasks were designed, which combined navigation and visual exploration in unknown scenarios and under different working conditions. Each participant had to perform two trials for each task. Task 1 involved complex navigation in constrained spaces with an active search for two visual targets. Task 2 involved navigation in open spaces with an active search for one visual target. The maps of the circuits are shown in Fig. 6. The maps were the only information of the remote environments shown to the participants, which had never been physically there. Regarding the stimulation process schedules, the interstimulus duration was set to 75 ms, and the stimulus duration was set to 125 ms. After each trial, the participants were asked to fill out neuropsychological and cognitive assessment forms, one for each operation mode of the system. The duration of this phase was 4 h per participant. It should be noted that execution of tasks was not counterbalanced (the two trials of Task 1 were performed before the trials of Task 2); thus, the obtained results containing intertask comparisons (particularly in the users' behavior evaluation) may reflect learning effects.

TABLE I
METRICS TO EVALUATE THE GLOBAL PERFORMANCE

	Task 1				Task 2			
	min	max	mean	std	min	max	mean	std
Task success	1	1	1	0	1	1	1	0
# collisions	0	0	0	0	0	0	0	0
Time (s)	685	1249	918	163	706	1126	910	154
Path length (m)	10.99	13.53	11.84	0.90	19.68	21.83	20.68	0.63
# missions	12	19	13.90	2.30	10	15	11.70	1.64
BCI accuracy	0.83	1.00	0.92	0.07	0.78	1.00	0.89	0.07
BCI select. ratio	0.46	0.60	0.53	0.05	0.45	0.59	0.52	0.05
Nav. ratio	0.65	0.77	0.70	0.04	0.70	0.86	0.78	0.04

IV. RESULTS AND EVALUATION

This section reports the results obtained during the experimental phases. Phase 1 was composed of a screening and a training task. Regarding the screening task, visual inspection of the recorded EEG data showed that the P300 potential was elicited for all participants. Furthermore, participants reported high satisfaction in the psychological assessments. Thus, the graphical interface design was validated. Regarding the training task, the pattern-recognition strategy was trained, and the participants performed the online tests. All participants achieved more than 93% BCI accuracy, and thus, all were qualified to carry out the next phase.

Phase 2 consisted of execution of the predefined teleoperation tasks, which combined navigation and visual exploration. First, the participants performed four offline trials to train the pattern-recognition strategy. The number of sequences was customized for each participant according to the results provided by the classifier in this calibration process (Fig. 4). The number of sequences was set to the minimal number that allowed the participant to achieve a theoretical accuracy higher than 90%. Then, the experiments were performed. Technical evaluation of the telepresence system and the behavior study of users are described next. The overall result was that all participants were able to complete the designed tasks, reporting no failures, which shows the robustness of the system and its feasibility to solve tasks in real settings where joint navigation and visual exploration were needed. Furthermore, participants showed great adaptation.

A. Technical Evaluation

The technical evaluation consisted of a global evaluation of the brain-actuated telepresence system and a particular evaluation of the brain–computer system and the robotic system.

1) Global Evaluation: Based on [5] and [38], the following metrics are proposed: 1) task success; 2) number of collisions of the navigation system; 3) time elapsed until completion of task; 4) length of path traveled by the robot; 5) number of missions[1] to complete the task; 6) BCI accuracy; 7) BCI selection ratio, which is the ratio between the time spent selecting orders and the total time to complete the task; and 8) navigation ratio, which is the ratio between the time spent in robot navigation mode and the total time to complete the task, which is com-

plementary to the exploration ratio. Results are summarized in Table I.

All participants succeeded to perform all trials, reporting no collisions and highlighting the robustness of the system. Time elapsed, path length, and number of missions were very similar for all participants, indicating similar performances among them (these metrics will be further discussed from the point of view of the participants in the users' behavior section). The real robot trajectories are shown in Fig. 6. Although there were variations in BCI accuracy, the BCI interaction was satisfactory as the BCI accuracy was always higher than 78%, achieving a mean performance of 90%. The BCI selection ratio was 52% on average, which shows the great importance of BCI accuracy in the global system performance. Regarding the ratio of usage of the operation modes, both operation modes were used to complete the tasks. It can also be inferred that the system provided enough functionalities to the users, so that they were able to adapt to the different working conditions of the tasks. Task 1 presented a higher exploration ratio because it involved more complex visual explorations. Task 2 presented a higher navigation ratio because it involved navigation in open spaces and simpler visual exploration.

In summary, results were very encouraging because they showed the feasibility of the technology to solve tasks combining navigation and visual exploration under different working conditions. Furthermore, participants were naïve to BCI usage and received a short briefing on the system operation. The system was calibrated in less than an hour.

2) Brain–Computer System: The evaluation of the brain–computer system was divided into two parts: evaluation of the pattern-recognition strategy performance (BCI accuracy) and evaluation of the visual display design. Based on [5] and [38], the following metrics are proposed: 1) total errors; 2) reusable errors; 3) real BCI accuracy; 4) practical BCI accuracy, which is the BCI accuracy computed using the correct selections plus reusable errors; 5) selections per minute; 6) selections per mission (usability rate); 7) missions per minute; 8) number of sequences; 9) ITR according to the Wolpaw definition[2] [39]; 10) number of errors caused by interface misunderstandings; and 11) option usage frequency. Results are summarized in Table II, except for the option usage frequency, which is shown in Table III.

---

[1]Missions are defined in the technology description (Section II) as an order sent to the robotic system (selection plus validation).

[2]$B = \log_2 N + P \log_2 P + (1 - P) \log_2 (1 - P/N - 1)$. B is the number of bits per trial (i.e., bits per selection), N is the number of possible selections, and P is the probability that a desired selection will occur.

TABLE II
METRICS TO EVALUATE THE BRAIN–COMPUTER SYSTEM

	Task 1				Task 2			
	min	max	mean	std	min	max	mean	std
# total errors	0.00	7.00	3.50	2.88	0.00	11.00	4.90	3.70
# reusable errors	0.00	2.00	0.60	0.84	0.00	5.00	1.20	1.81
Real BCI acc.	0.81	1.00	0.90	0.08	0.73	1.00	0.86	0.09
Practical BCI acc.	0.83	1.00	0.92	0.07	0.78	1.00	0.89	0.07
# selections/min	3.39	5.49	4.41	0.72	3.40	4.77	4.16	0.46
# selections/mission	2.11	3.08	2.54	0.34	2.36	3.40	2.80	0.39
# missions/min	1.17	2.27	1.77	0.39	1.00	2.02	1.53	0.33
# sequences	6.00	10.00	8.00	1.33	8.00	10.00	8.40	0.84
ITR (bits/min)	9.97	21.73	16.05	3.83	9.86	20.62	14.32	3.33
# misunderstandings	0.00	0.00	0.00	0.00	0.00	1.00	0.10	0.32

TABLE III
METRICS TO EVALUATE THE OPTION USAGE FREQUENCY

		Task 1				Task 2			
		min	max	mean	std	min	max	mean	std
Nav.mode	# 1st grid row	0.00	2.00	1.40	0.84	2.00	6.00	4.70	1.16
	# 2nd grid row	1.00	6.00	3.00	1.63	0.00	7.00	2.10	2.02
	# 3rd grid row	0.00	2.00	0.90	0.57	0.00	2.00	1.10	0.57
	# turn left	0.00	3.00	1.60	1.07	0.00	2.00	0.70	0.82
	# turn right	1.00	3.00	2.10	0.88	0.00	1.00	0.10	0.32
	# refresh	0.00	2.00	0.50	0.71	0.00	1.00	0.10	0.32
	# change	1.00	1.00	1.00	0.00	1.00	1.00	1.00	0.00
Exp.mode	# 1st grid row	1.00	2.00	1.40	0.52	2.00	3.00	2.20	0.42
	# 2nd grid row	1.00	4.00	2.80	1.03	0.00	1.00	0.10	0.32
	# 3rd grid row	0.00	2.00	0.40	0.70	0.00	1.00	0.30	0.48
	# alignment	0.00	1.00	0.30	0.48	0.00	1.00	0.30	0.48
	# home	0.00	0.00	0.00	0.00	0.00	1.00	0.10	0.32
	# refresh	0.00	1.00	0.20	0.42	0.00	0.00	0.00	0.00
	# change	0.00	1.00	0.70	0.48	0.00	1.00	0.70	0.48

a) BCI accuracy evaluation: Participants were instructed to report an error to the experimenter through a small movement of the right-hand index finger. In some cases, although the BCI detects an undesired target, the target is reused to complete the task (common situation in open spaces, where a task can be solved in many different ways). These errors are referred to as reusable errors, and they do not increment the time to set a mission to the system. The distinction between a reusable error and a nonreusable error was made by the experimenter and then verified with the participants at the end of the experiment (when needed). Real BCI accuracy was high, above 85% on average. Reusable errors result in a practical BCI accuracy higher than real. Practical accuracy was 90% on average. The BCI system set only two incorrect missions in all executions, representing 0.78% of all missions (the theoretical probability of this situation was 0.3%). The number of sequences was customized per participant according to their accuracy, between six and ten. The number of sequences determined the number of selections per minute, which was approximately four. The usability rate was slightly greater than two (ideally, it is equal to two, i.e., a mission needs at least one selection plus validation) due to BCI errors and interface misunderstandings by the user. The number of missions per minute, determined by the number of selections per minute and the usability rate, was 1.65 on average. The ITR of the BCI system was 15 b/min on average.

b) Visual display design evaluation: The design of the interface was valid, as participants achieved tasks with only a short briefing on its functionalities. There was only one incorrect selection due to interface misunderstandings, which arose at the very end of one trial (the participant set an unreachable mission, located behind the goal wall). The usage frequency for all options in the interface and participants shows that all functionalities were used, thus indicating that there were no useless options. Furthermore, it also suggests a usable visual display design. The change mode option was used once per trial in each operation mode due to the requirements of the designed tasks (participants changed to the exploration mode to visualize the targets and then switched to navigation mode to complete the tasks). Note that alignment and change mode options in the exploration mode were complementary, since both options allowed the participant to change to the navigation mode. The home option in the exploration mode was used only once throughout all the experiments, probably because, in the predefined tasks, the home option did not provide an important advantage with regard to grid destinations. The refresh option was little used because of the execution of constrained tasks; this option could be useful in more uncontrolled tasks to increase the interaction capabilities.

In summary, these results show a satisfactory integration between the visual display and the designed stimulation process as the participants successfully completed all trials with high BCI accuracies. Furthermore, the graphical interface was usable and easy to understand. The system presents low ITRs, which is a common problem of all event-related potential approaches, but it is in part overcome by the adoption of a shared-control approach.

3) Robotic System: Based on [5] and [38], the following set of metrics is proposed to evaluate the two operation modes of the robotic system: 1) number of navigation missions; 2) length traveled per mission; 3) mean velocity of the robot; 4) mean

TABLE IV
METRICS TO EVALUATE THE ROBOTIC SYSTEM

		Task 1				Task 2			
		min	max	mean	std	min	max	mean	std
Nav.	# missions	7.00	12.00	9.00	1.60	7.00	11.00	8.70	1.20
	Length (m)/mission	1.06	1.61	1.34	0.18	1.90	2.81	2.41	0.29
	Velocity (m/s)	0.05	0.07	0.06	0.01	0.08	0.10	0.10	0.01
	Clearance mean (m)	0.89	1.12	1.03	0.07	1.09	1.19	1.14	0.03
	Clearance min (m)	0.32	0.52	0.45	0.05	0.41	0.62	0.52	0.07
Exp.	# missions	4.00	7.00	4.90	1.20	2.00	5.00	3.00	1.10
	Exploration (rad)	1.21	6.37	2.79	1.56	0.16	0.88	0.37	0.25

TABLE V
METRICS FOR THE EXECUTION ANALYSIS

		P1		P2		P3		P4		P5	
		Tr.1	Tr.2	Tr.1	Tr.2	Tr.1	Tr.2	Tr.1	Tr.2	Tr.1	Tr.2
Task 1	Task success	1	1	1	1	1	1	1	1	1	1
	# missions	13.00	12.00	19.00	12.00	12.00	15.00	12.00	14.00	16.00	14.00
	Path length (m)	11.30	11.97	13.34	11.36	10.99	11.61	11.04	13.53	11.37	11.94
	Time (s)	807	685	1249	1022	798	962	963	1039	860	792
	Pract. BCI acc.	0.89	0.97	1.00	0.83	0.97	0.89	0.84	0.85	0.97	1.00
Task 2	Task success	1	1	1	1	1	1	1	1	1	1
	# missions	10.00	15.00	13.00	10.00	11.00	12.00	12.00	13.00	11.00	10.00
	Path length (m)	20.72	21.12	21.83	20.86	19.68	20.78	19.93	20.88	20.09	20.86
	Time (s)	884	1045	1126	1015	742	827	949	1073	729	706
	Pract. BCI acc.	0.88	0.92	0.92	0.82	0.92	0.90	0.78	0.83	1.00	0.96

clearance (average of the minimum distances to the obstacles); 5) minimum clearance (minimum distance to the obstacles); 6) number of camera exploration missions; and 7) total angle explored by the camera. Results are summarized in Table IV, which is divided into two sections, each relevant to an operation mode.

Regarding the navigation mode, a total of 177 navigation missions was carried out without collisions, with a total length of 325 m and a mean velocity of 0.08 m/s (10 times less than usual human walking velocity). The mean velocity and length traveled per mission were greater in Task 2 than in Task 1, which denotes that the navigation system was able to deal with the different environmental conditions, resulting in a velocity increase in open spaces (Task 2) and a reduction when maneuverability became more important (Task 1). Mean and minimum clearances show that the vehicle carried out obstacle avoidance with safety margins, which is one of the typical difficulties in autonomous navigation [34]. Regarding the exploration mode, a total of 79 missions was carried out, exploring a total angular distance of 3.2 rad.

In general, the performance of the robotic system was remarkable as the navigation missions were successfully executed, reporting no failures. The exploration system provided a good visual feedback of the remote environment and sufficient functionalities for active exploration.

B. Users' Behavior Evaluation

An evaluation of the users' behavior was carried out to measure the degree of participant adaptability to the brain-actuated telepresence system. Three studies were defined to achieve such an objective: 1) execution analysis, to study the performance of participants; 2) activity analysis, to study the interaction strategy with the robot; and 3) psychological assessment, to study the participants' workload, learnability, and level of confidence.

1) Execution Analysis: A set of metrics based on [5] and [38] was used: 1) task success; 2) number of missions; 3) path

length traveled by the robot; 4) time elapsed until completion of task; and 5) practical BCI accuracy. Results are summarized in Table V, which shows the two trials per participant and task.

The number of missions is an indicator of the intermediate steps required to complete the tasks. Although this metric is strongly related to the interaction strategy (discussed in the next section), it can be inferred that some participants presented a more efficient mission selection. Participants 1 and 4 showed a more efficient mission selection in Task 1, while participants 2, 3, and 5 presented a more efficient selection in Task 2. This metric suggests that these participants could be divided into two groups, according to the way that they adapted to the environmental conditions. One group adapted better to the constrained environment of Task 1, and the other group adapted better to the open spaces in Task 2. Path length is another metric of individual performance in the use of the telepresence system. Participants 3 and 5 presented shorter path lengths in both tasks, showing a better adaptation to the automation capabilities of the system. Execution time involves BCI accuracy and mission selection performance, which are factors that can increase the number of selections required to complete the tasks. Due to the large amount of time needed to select an option with the BCI (13 s on average), the lower BCI accuracies lead to the longer execution times. Participants 2 and 4 presented lower BCI accuracies and, consequently, longer execution times. The fact that all participants succeeded in completing the tasks shows that all participants successfully adapted to the system, which is a good indicative to explore the transition of the technology toward end users.

2) Activity Analysis: The interaction strategy of the participants when teleoperating the robot is studied. Regarding robotic devices that provide automation facilities, two types of interaction strategies can be applied: supervisory-oriented interaction and direct-control-oriented interaction [40]. Supervisory-oriented interaction extensively explores the automation capabilities (mainly trajectory planning and obstacle avoidance in navigation mode) minimizing user intervention.

TABLE VI
METRICS FOR THE ACTIVITY ANALYSIS

	Task 1				Task 2			
	min	max	mean	std	min	max	mean	std
D_A	-0.04	0.22	0.08	0.09	0.17	0.44	0.31	0.09
P_M	1.06	1.61	1.34	0.18	1.90	2.81	2.41	0.29
T_M	17.36	26.12	21.36	2.62	21.64	28.14	25.34	2.16
C_A	0.08	0.23	0.16	0.06	0.00	0.12	0.03	0.04
S_A	0.00	0.11	0.07	0.04	0.08	0.32	0.21	0.08

Direct-control-oriented interaction is characterized by an increased user intervention, minimizing the use of automation capabilities. In the concrete case of the developed system, supervisory-oriented interaction will be characterized by a high number of far destinations in the navigation, while direct-control-oriented interaction will be characterized by a higher number of near-range destinations or left-/right-turn selections.

The following metrics, adapted from [5] and [38], were defined to study whether the participants followed different interaction strategies in the two tasks: activity discriminant (D_A), which is the ratio between goal selections minus total of turn selections and the total number of selections; (P_M) path length per mission; robot motion time per mission (T_M); control activity descriptor (C_A), which is the ratio between turn selections and total number of selections; supervisory activity descriptor (S_A), which is the ratio between the first grid row destinations and total number of selections. According to the proposed metrics, high values of activity discriminant (D_A), path length per mission (P_M), and robot motion time per mission (T_M) indicate a tendency toward supervisory-oriented interaction. On the contrary, low values indicate a tendency toward control-oriented interaction. Furthermore, control-oriented interaction is also characterized by high values of C_A, whereas supervisory interaction is characterized by high values of S_A. Results are summarized in Table VI.

Values of D_A, P_M, and T_M in Task 1 were comparatively lower than those in Task 2, suggesting control interaction in Task 1 and supervisory interaction in Task 2. In Task 1, participants exhibited a propensity toward control interaction as C_A values were higher in comparison to the values in Task 2. In Task 2, participants showed a propensity toward supervisory interaction as S_A values were higher in comparison to those in Task 1. In summary, these results suggest that the participants adapted to the different working conditions of each task. Task 1 involved complex maneuverability, and participants presented control-oriented interaction; Task 2 involved more simple navigation in open spaces, and participants presented supervisory-oriented interaction.

3) Psychological Assessment: This section studies the adaptability of the participants to the telepresence system from a psychological point of view. The following metrics were used: 1) workload based on effort, which is the amount of effort exerted by the participant during the tasks; 2) learnability, which is the easiness to learn how to use the system during the tasks; and 3) level of confidence, which is the confidence experienced by the participant during the tasks. The results obtained from the questionnaires (filled out after each trial by the participants) are shown in Fig. 7.
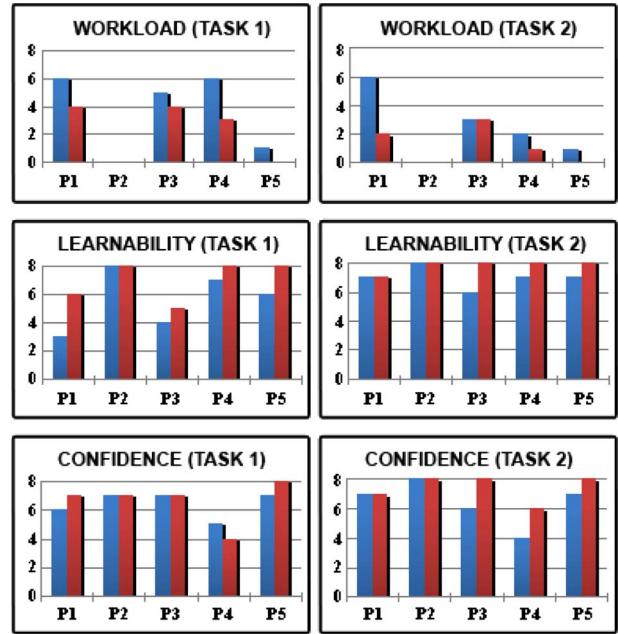

Fig. 7. Metrics used for the psychological assessment in the two teleoperation tasks. The first bar represents trial 1, and the second bar represents trial 2. The value for each metric in each trial of a task is the sum of two questionnaires values in a [0–4] scale, one for each operation mode (those values have been grouped as no differences were found between the two modes). Workload assessment is on a [0–8] scale, from almost no effort to considerable effort. Learnability assessment is on a [0–8] scale, from difficult to easy to learn. The level of confidence assessment is on a [0–8] scale, from least confident to highly confident.

Participants 2 and 5 reported less workload than participants 1, 3, and 4. All participants reported higher values of workload in Task 1. This result might be due to the fact that Task 1 involved more complex maneuverability. Regarding the learnability metric, participant 1 presented difficulties in learning how to solve the first task but showed a great improvement in Task 2. This participant may have initially found the telepresence system complex. Regarding the level of confidence, participant 4 showed the lowest values, which might be explained by his low BCI accuracy (see Table V). In general, these three metrics showed a great improvement in Task 2 with regard to Task 1. An improvement in metrics can be observed in the second trial with regard to the first one (within each task), where the first trial may be seen as an adaptation trial to complete the new task. These results suggest high adaptability of the participants to the telepresence system: Participants experienced less effort and higher learning skills and felt more confident during the use of the system. However, these results should be interpreted with caution since tasks were not counterbalanced, and thus, they may reflect a learning effect.

V. CONCLUSION

This paper has reported a synchronous P300-based BCI teleoperation system that can provide users with presence in remote environments through a mobile robot, both connected via the Internet. The shared-control strategy is built by the BCI decoding of task-related navigation or visual exploration orders, autonomously executed by the robot. This design overcomes

low ITRs, avoids exhausting mental processes, and explicitly avoids delay problems in the control loop caused by Internet communication (as what happens in teleoperation systems with continuous control).

All users participating in the experimental methodology were able to accomplish two different tasks, which covered typical navigation situations such as complex maneuverability and navigation in open spaces. The interaction with the BCI was satisfactory as naïve BCI users obtained high accuracies (88% in mean) with short calibration time (less than an hour). The functionalities of the robotic system were sufficient to complete the tasks. The navigation system implemented task-level primitives that incorporated real-time adaptive motion planning and model construction, and thus, it was able to deal with nonpreprogrammed and populated scenarios. As demonstrated in other applications [5], [38], the navigation system demonstrated to be robust (the robot received 177 missions without any failure). The integration between the BCI system and the robotic system was satisfactory, achieving an overall high performance of the system. The evaluation of the users' behavior suggested a high degree of adaptability to the telepresence system.

One feature of the current system is that no continuous feedback is perceived when the user is interacting with the BCI. With this feature, the user is never exposed to external stimuli while interacting with the BCI, and thus, it allows one to employ a methodology to explore the BCI accuracy in controlled scenarios. However, this certainly limits the degree of presence and shared-control interaction, and further investigation is required to understand the effects that the alleviation of this restriction could have. In order to increase the degree of presence, the adoption of an asynchronous P300 control to support an idle state would be an improvement, as given in [41]. Another improvement could be the adoption of a multiparadigm BCI by the inclusion of an asynchronous error-potential detection protocol [42]. This improvement could have two effects. On one hand, this could reduce the interaction required by the BCI to control the robot (note that 50% of the total time is spent in decoding the BCI intentions due the safety nature of the device, implemented in the execution protocol through a validation step) by removing the validation protocol as incorrect P300 selections could be detected. On the other hand, the inclusion of this protocol could increase the shared-control interaction and system safety by detecting possible unrecognized risks by the robot's sensors while navigating. However, the adoption of such solutions could impose the typical drawbacks of asynchronous protocols: lower accuracies, much higher calibration and training time with the user, and higher cognitive effort.
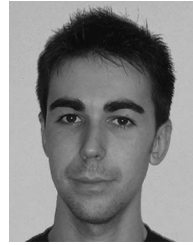
This study could be considered as a step toward the development of new telepresence-oriented systems using BCIs and mobile robots in which navigation and visual exploration problems are solved. Thus, it could allow the designers to focus on specific interaction functionalities (e.g., incorporate bidirectional communication along the lines of a video conference), which might be dependent on the patient pathology and needs. Although the utility of this technology was demonstrated for healthy users, the final objective is to bring these possibilities closer to patients with neuromuscular disabilities, which is the direction of work in the near future [28].

REFERENCES

[1] J. R. Wolpaw, D. J. McFarland, G. W. Neat, and C. A. Forneris, "An EEG-based brain–computer interface for cursor control," *Electroencephalography Clin. Neurophysiol.*, vol. 78, no. 3, pp. 252–259, Mar. 1991.

[2] N. Birbaumer, N. Ghanayim, T. Hinterberger, I. Iversen, B. Kotchoubey, A. Kübler, J. Perelmouter, E. Taub, and H. Flor, "A spelling device for the paralyzed," *Nature*, vol. 398, no. 6725, pp. 297–298, Mar. 1999.

[3] A. A. Karim, T. Hinterberger, J. Richter, J. Mellinger, N. Neumann, H. Flor, A. Kübler, and N. Birbaumer, "Neural Internet: Web surfing with brain potentials for the completely paralyzed," *Neurorehab. Neural Repair*, vol. 20, no. 4, pp. 508–515, Dec. 2006.

[4] J. R. Millán, F. Renkens, J. Mouriño, and W. Gerstner, "Noninvasive brain-actuated control of a mobile robot by human EEG," *IEEE Trans. Biomed. Eng.*, vol. 51, no. 6, pp. 1026–1033, Jun. 2004.

[5] I. Iturrate, J. M. Antelis, A. Kübler, and J. Minguez, "A noninvasive brain-actuated wheelchair based on a P300 neurophysiological protocol and automated navigation," *IEEE Trans. Robot.*, vol. 25, no. 3, pp. 614–627, Jun. 2009.

[6] G. Vanacker, J. R. Millán, E. Lew, P. W. Ferrez, F. G. Moles, J. Philips, H. Van Brussel, and M. Nuttin, "Context-based filtering for assisted brain-actuated wheelchair driving," *Comput. Intell. Neurosci.*, vol. 2007, p. 3, Jan. 2007.

[7] T. Luth, D. Ojdanic, O. Friman, O. Prenzel, and A. Graser, "Low level control in a semi-autonomous rehabilitation robotic system via a brain–computer interface," in *Proc. IEEE 10th ICORR*, 2007, pp. 721–728.

[8] B. Rebsamen, E. Burdet, C. Guan, H. Zhang, C. L. Teo, Q. Zeng, C. Laugier, and M. H. Ang, Jr., "Controlling a wheelchair indoors using thought," *IEEE Intell. Syst.*, vol. 22, no. 2, pp. 18–24, Mar./Apr. 2007.

[9] A. Ferreira, W. C. Celeste, F. A. Cheein, T. F. Bastos-Filho, M. Sarcinelli-Filho, and R. Carelli, "Human–machine interfaces based on EMG and EEG applied to robotic systems," *J. NeuroEng. Rehab.*, vol. 5, no. 1, pp. 1–15, Mar. 2008.

[10] I. Iturrate, L. Montesano, and J. Minguez, "Single trial recognition of error-related potentials during observation of robot operation," in *Proc. Int. Conf. IEEE EMBC*, 2010, pp. 4181–4184.

[11] C. J. Bell, P. Shenoy, R. Chalodhorn, and R. P. N. Rao, "Control of a humanoid robot by a noninvasive brain–computer interface in humans," *J. Neural Eng.*, vol. 5, no. 2, pp. 214–220, Jun. 2007.

[12] G. Pfurtscheller, G. R. Müller, J. Pfurtscheller, H. J. Gerner, and R. Rupp, ""Thought"—Control of functional electrical stimulation to restore hand grasp in a patient with tetraplegia," *Neurosci. Lett.*, vol. 351, no. 1, pp. 33–36, Nov. 2003.

[13] M. Tavella, R. Leeb, R. Rupp, and J. R. Millán, "Towards natural noninvasive hand neuroprostheses for daily living," in *Proc. Int. Conf. IEEE EMBC*, 2010, pp. 126–129.

[14] A. Chella, E. Pagello, E. Menegatti, R. Sorbello, S. M. Anzalone, F. Cinquegrani, L. Tonin, F. Piccione, K. Prifitis, C. Blanda, E. Buttita, and E. Tranchina, "A BCI teleoperated museum robotic guide," in *Proc. Int. Conf. CISIS*, 2009, pp. 783–788.

[15] A. Akce, M. Johnson, and T. Bretl, "Remote teleoperation of an unmanned aircraft with a brain–machine interface: Theory and preliminary results," in *Proc. IEEE ICRA*, 2010, pp. 5322–5327.

[16] L. Tonin, E. Menegatti, M. Cavinato, C. Avanzo, M. Pirini, A. Merico, L. Piron, K. Priftis, S. Silvoni, C. Volpato, and F. Piccione, "Evaluation of a robot as embodied interface for brain computer interface systems," *Int. J. Bioelectromagn.*, vol. 11, no. 2, pp. 97–104, 2009.

[17] L. Tonin, R. Leeb, M. Tavella, S. Perdikis, and J. R. Millán, "The role of shared-control in BCI-based telepresence," in *Proc. IEEE Int. Conf. SMC*, 2010, pp. 1462–1466.

[18] A. Kübler and N. Birbaumer, "Brain–computer interfaces and communication in paralysis: Extinction of goal directed thinking in completely paralysed patients?," *Clin. Neurophysiol.*, vol. 119, no. 11, pp. 2658–2666, Nov. 2008.

[19] F. Galán, M. Nuttin, E. Lew, P. W. Ferrez, G. Vanacker, J. Philips, and J. R. Millán, "A brain-actuated wheelchair: Asynchronous and non-invasive brain–computer interfaces for continuous control of robots," *Clin. Neurophysiol.*, vol. 119, no. 9, pp. 2159–2169, Sep. 2008.

[20] J. R. Wolpaw, N. Birbaumer, D. J. McFarland, G. Pfurtscheller, and T. M. Vaughan, "Brain–computer interfaces for communication and control," *Clin. Neurophysiol.*, vol. 113, no. 6, pp. 767–791, 2002.

[21] J. Minguez, F. Lamiraux, and J. P. Laumond, "Motion planning and obstacle avoidance," in *Springer Handbook of Robotics*, B. Siciliano and O. Khatib, Eds. Berlin, Germany: Springer-Verlag, 2008, pp. 827–852.

[22] C. Escolano, J. M. Antelis, and J. Minguez, "Human brain-teleoperated robot between remote places," in *Proc. IEEE ICRA*, 2009, pp. 4430–4437.

[23] S. Sutton, M. Braren, J. Zublin, and E. R. John, "Evoked potential correlates of stimulus uncertainty," *Science*, vol. 150, no. 3700, pp. 1187–1188, Nov. 1965.

[24] S. H. Patel and P. N. Azzam, "Characterization of N200 and P300: Selected studies of the event-related potential," *Int. J. Med. Sci.*, vol. 2, no. 4, pp. 147–154, 2005.

[25] J. R. Millán, R. Rupp, G. R. Müller-Putz, R. Murray-Smith, C. Giugliemma, M. Tangermann, C. Vidaurre, F. Cincotti, A. Kübler, R. Leeb, C. Neuper, K. R. Müller, and D. Mattia, "Combining brain–computer interfaces and assistive technologies: State-of-the-art and challenges," *Frontiers Neurosci.*, vol. 4, p. 161, 2010.

[26] D. J. Krusienski, E. W. Sellers, F. Cabestaing, S. Bayoudh, D. J. McFarland, T. M. Vaughan, and J. R. Wolpaw, "A comparison of classification techniques for the P300 speller," *J. Neural Eng.*, vol. 3, no. 4, pp. 299–305, Dec. 2006.

[27] G. Schalk, D. J. McFarland, T. Hinterberger, N. Birbaumer, and J. R. Wolpaw, "BCI2000: A general-purpose brain–computer interface (BCI) system," *IEEE Trans. Biomed. Eng.*, vol. 51, no. 6, pp. 1034–1043, Jun. 2004.

[28] C. Escolano, A. Ramos, T. Matuz, N. Birbaumer, and J. Minguez, "A telepresence robotic system operated with a P300-based brain–computer interface: Initial tests with ALS patients," in *Proc. Int. Conf. IEEE EMBC*, 2010, pp. 4476–4480.

[29] L. A. Farwell and E. Donchin, "Talking off the top of your head: Toward a mental prosthesis utilizing event-related brain potentials," *Electroencephalography Clin. Neurophysiol.*, vol. 70, no. 6, pp. 510–523, Dec. 1988.

[30] D. J. Krusienski, E. W. Sellers, D. J. McFarland, T. M. Vaughan, and J. R. Wolpaw, "Toward enhanced P300 speller performance," *J. Neurosci. Methods*, vol. 167, no. 1, pp. 15–21, Jan. 2008.

[31] T. H. J. Collett, B. A. MacDonald, and B. P. Gerkey, "Player 2.0: Toward a practical robot programming framework," in *Proc. ACRA*, 2005.

[32] L. Montesano, J. Minguez, and L. Montano, "Modeling dynamic scenarios for local sensor-based motion planning," *Auton. Robots*, vol. 25, no. 3, pp. 231–251, Oct. 2008.

[33] J. Minguez and L. Montano, "Sensor-based robot motion generation in unknown, dynamic and troublesome scenarios," *Robot. Auton. Syst.*, vol. 52, no. 4, pp. 290–311, Sep. 2005.

[34] L. Montesano, J. Minguez, and L. Montano, "Lessons learned in integration for sensor-based robot navigation systems," *Int. J. Adv. Robot. Syst.*, vol. 3, no. 1, pp. 85–91, 2006.

[35] A. Ranganathan and S. Koenig, "A reactive robot architecture with planning on demand," in *Proc. IEEE Int. Conf. IROS*, 2003, pp. 1462–1468.

[36] J. Minguez and L. Montano, "Nearness diagram (ND) navigation: Collision avoidance in troublesome scenarios," *IEEE Trans. Robot. Autom.*, vol. 20, no. 1, pp. 45–59, Feb. 2004.

[37] J. Minguez and L. Montano, "Extending collision avoidance methods to consider the vehicle shape, kinematics, and dynamics of a mobile robot," *IEEE Trans. Robot.*, vol. 25, no. 2, pp. 367–381, Apr. 2009.

[38] L. Montesano, M. Diaz, S. Bhaskar, and J. Minguez, "Towards an intelligent wheelchair system for users with cerebral palsy," *IEEE Trans. Neural Syst. Rehabil. Eng.*, vol. 18, no. 2, pp. 193–202, Apr. 2010.

[39] J. R. Wolpaw, N. Birbaumer, W. J. Heetderks, D. J. McFarland, P. H. Peckham, G. Schalk, E. Donchin, L. A. Quatrano, C. J. Robinson, and T. M. Vaughan, "Brain–computer interface technology: A review of the first international meeting," *IEEE Trans. Rehabil. Eng.*, vol. 8, no. 2, pp. 164–173, Jun. 2000.

[40] M. Baker, R. Casey, B. Keyes, and H. A. Yanco, "Improved interfaces for human–robot interaction in urban search and rescue," in *Proc. IEEE Int. Conf. SMC*, 2004, pp. 2960–2965.

[41] H. Zhang, C. Guan, and C. Wang, "Asynchronous P300-based brain–computer interfaces: A computational approach with statistical models," *IEEE Trans. Biomed. Eng.*, vol. 55, no. 6, pp. 1754–1763, Jun. 2008.

[42] A. Buttfield, P. W. Ferrez, and J. R. Millán, "Towards a robust BCI: Error potentials and online learning," *IEEE Trans. Neural Syst. Rehabil. Eng.*, vol. 14, no. 2, pp. 164–168, Jun. 2006.

Carlos Escolano received the B.S. degree in computer science and the M.Sc. degree from the Universidad de Zaragoza, Zaragoza, Spain, in 2008 and 2010, respectively. He is currently working toward the Ph.D. degree in brain–computer interfaces in the Robotics, Perception and Real Time Group, Universidad de Zaragoza. He initiated research on brain–computer interfaces within the framework of his M.Sc. thesis in 2007, being responsible for software engineering tasks during the development of a brain-actuated telepresence mobile robot.

His research interests are brain–computer interfaces, software engineering applied to brain–computer interfaces, and neurofeedback.

Javier Mauricio Antelis received the B.S. degree in electronic engineering from Francisco de Paula Santander University, Cúcuta, Colombia, the M.Sc. degree in electronic systems from the Instituto Tecnologico de Monterrey, Monterrey, Mexico, and the M.Sc. degree in biomedical engineering from the Universidad de Zaragoza, Zaragoza, Spain, where he is currently working toward the Ph.D. degree in biomedical engineering.

He was an Assistant Researcher with the Mechatronics Automotive Research Center, Toluca, Mexico, and was a visiting graduate student at the Institute of Medical Psychology and Behavioural Neurobiology, Tubingen, Germany. His research interests include noninvasive brain–computer interfaces, the dynamic electroencephalogram (EEG) source localization problem, and the recognition of cognitive states from EEG signals and electrophysiological recordings using advanced signal processing techniques, estimation theory, Bayesian inference, and sequential Monte Carlo methods.

Javier Minguez received B.S. degree in physics science from the Universidad Complutense de Madrid, Madrid, Spain, in 1996 and the Ph.D. degree in computer science and systems engineering from the Universidad de Zaragoza, Zaragoza, Spain, in 2002.

He has been an Invited Researcher with the Robotics and Artificial Intelligence Group, Laboratoire d'Analyse et d'Architecture des Systèmes, Centre National de la Recherche Scientifique, Toulouse, France; the Robot and Computer Vision Laboratory, Instituto de Sistemas e Robótica, Instituto Superior Técnico, Technical University of Lisbon, Lisbon, Portugal; the Robotics Laboratory, Stanford University, Stanford, CA; and the Institute of Medical Psychology and Behavioural Neurobiology, Tubingen, Germany. Since 2008, he has been an Associate Professor with the Robotics, Perception and Real Time Group, Universidad de Zaragoza, where he is the Leader of the Neurotechnology Research Team. His research interest includes the synergy between neural interfaces and robotics.